

Lateral tension increases the line tension between two domains in a lipid bilayer membraneSergey A. Akimov,^{1,2} Peter I. Kuzmin,^{1,2} Joshua Zimmerberg,² and Fredric S. Cohen³¹*Laboratory of Bioelectrochemistry, Frumkin Institute of Physical Chemistry and Electrochemistry, Russian Academy of Sciences, Moscow, Russia 119991*²*Laboratory of Cellular and Molecular Biophysics, National Institute of Child Health and Human Development, National Institutes of Health, Bethesda, Maryland 20892, USA*³*Department of Molecular Biophysics and Physiology, Rush University Medical Center, Chicago, Illinois 60612, USA*

(Received 4 October 2006; published 18 January 2007)

The effect of an external applied lateral tension on the line tension between two domains of different thickness in a lipid bilayer membrane is calculated. The thick domain is treated as a liquid-ordered phase in order to model a raft in a biological membrane; the thin domain is considered a liquid-disordered phase to model the surrounding region. In our model, the monolayers elastically distort at the boundary to create a smooth rather than steplike boundary to avoid exposure of the hydrophobic interior of the thick raft to water. The energy of this distortion is described by the fundamental deformations of splay and tilt. This energy per unit length of boundary yields the line tension of the raft. Applying lateral tension alters the fundamental deformations such that line tension increases. This increase in line tension is larger when the spontaneous curvature of a raft is greater than that of the surround; if the spontaneous curvature of the raft is less than that of the surround, the increase of the line tension due to application of the lateral tension is more modest.

DOI: [10.1103/PhysRevE.75.011919](https://doi.org/10.1103/PhysRevE.75.011919)

PACS number(s): 87.14.Cc, 87.17.-d

I. INTRODUCTION

The activity of many membrane proteins is regulated by their lipid environment. Binding of specific lipids to proteins is one regulatory mechanism. There are also at least two mechanisms for this regulation that are not contingent upon direct lipid binding: (1) integral membrane proteins may be strongly affected by the physical and chemical properties of the immediately surrounding lipids; [1–3] (2) the activation of proteins that interact with other can be enhanced if they all reside in the same small domain. [4,5] Because protein function can be dependent upon their location, there is much interest in lipid domains in biological and model membranes. In lipid bilayer membranes, cholesterol and sphingomyelin can definitely form domains by phase separation. These domains can merge to very large sizes, on the order of many micrometers. [6] There is considerable evidence that such domains also exist in biological plasma membranes, but if they do, they remain small. [7] Small size has been an experimental detriment for definitively ascertaining whether rafts do exist in biological membranes. Some proteins thought to reside in rafts definitely move along the plane of a membrane as if they remain in a relatively stable domain (i.e., it exists for a long time) of diameter ~ 30 nm. [7] This domain thus appears to move along the plane of the membrane as if it were a “raft.” [8] Rafts have been implicated in cell processes as diverse as signal transduction [3,4,9,10], endocytosis [11–13], intracellular trafficking [14,15], and membrane fusion [7]. Because the rafts are small in biological membranes, they are not only difficult to identify but their physical properties have not been measured, although physical properties of domains in lipid bilayers that are thought to model rafts have been determined. Atomic force microscopy has consistently shown that these domains are thicker than the surrounding membrane [16,17]. This difference in thickness, known as “height mismatch,” can be a

dominant contributor to the boundary energy or “line tension” of the domain [18].

Conditions have been found in which cholesterol and sphingomyelin phase separate in lipid bilayers to form nanoscopic-sized rafts that do not merge to large sizes [19–22]. Merger lowers the total length of the boundary of the merged domains and thus lowers the boundary energy. The higher the line tension, the greater is the lowering of boundary energy upon raft merger, but this favorable lowering of free energy upon merger is opposed by the resulting decrease in entropy of the raft ensemble. The decrease in entropy that results from the smaller number of rafts after merger is independent of line tension. As a result, physical and chemical forces that regulate the value of line tension can determine whether rafts merge and this can control the size distribution of rafts [23]. Experimentally, application of lateral tension to a giant unilamellar vesicle (GUV) promotes the creation of micrometer-sized rafts [24]. We previously developed a theory that predicts the line tension of a raft having a thickness greater than that of the surrounding bilayer [25]. The calculated value of raft line tension depended on physical parameters such as the degree of height mismatch, the elastic moduli, and the spontaneous curvatures of the raft and surrounding bilayer. The consequences of lateral tension were not considered. In the present study we generalize the theory and show that line tension increases upon application of a lateral tension.

II. STATEMENT OF THE PROBLEM

If a raft and the surrounding membrane were unperturbed at their boundary, a height mismatch would lead to the exposure of the hydrophobic membrane interior to water [Fig. 1(a)]. A simple estimation shows that the energy of such exposure (per unit length of the boundary) is extremely high, ~ 20 – 40 pN for a height mismatch of ~ 0.5 – 1 nm. This is

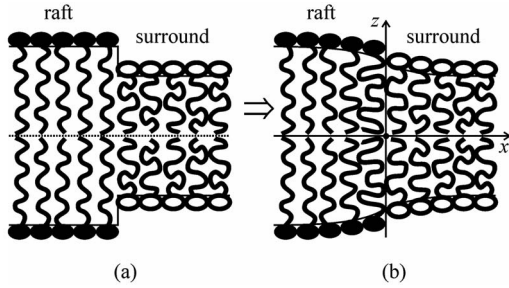


FIG. 1. Compensation of hydrophobic mismatch by elastic deformations of a membrane. (a) Initially, there is a steplike boundary where a thick (raft) and thin bilayer (surround) meet. This causes significant exposure of a hydrophobic surface to water. (b) The hydrophobic core of the membrane is sequestered from water after the monolayers elastically deform near the boundary. The Ox and Oz axes of the Cartesian coordinate system are shown. The Oy axis (not shown) projects into the plane of the figure.

much greater than experimentally estimated values, ~ 1 pN, of line tension [24]. To reduce the boundary energy, the thicker membrane (raft) will deform near its boundary to decrease its thickness, and the thinner membrane (surround) will deform to increase its thickness so that hydrophobic exposure of bilayer interior to water is prevented. In our model, the line tension of a raft is the mechanical energy per unit length of boundary necessary for the membrane to elastically deform to the extent that height mismatch is eliminated at the boundary [Fig. 1(b)].

A. Setting up the system

We analyze a bilayer that consists of two identical monolayers [Fig. 1(b)]. Because these monolayers exhibit mirror symmetry relative to the monolayer interfaces (i.e., the mid-plane of the bilayer), we can consider a single monolayer with a planar interface. We treat the raft and the surrounding region as a semi-infinite monolayer sheet, placing the raft on the left and the surround on the right (see Fig. 1). The boundary is approximated as a straight line when viewed from the top of the monolayer. This approximation is valid for a raft radius that is large compared to the characteristic length of the deformations, which is usually about several nanometers. Quantitatively, we describe this monolayer by a Cartesian coordinate system with origin O at the raft boundary. The Ox axis is in the plane of the interface of the monolayer and is directed perpendicular to the raft boundary and into the surround; the Oy axis is directed along the boundary; the Oz axis is perpendicular to the plane of the monolayer interface [Fig. 1(b)]. (The origin of this coordinate system, and the Oy axis, are not shown.) The system is invariant to translations along the Oy axis. In short, the raft is the $x < 0$ region, the surround is the $x > 0$ region, and the boundary is located at $x = 0$.

We treat the monolayer as a continuous elastic anisotropic medium having a hydrophobic interior that is everywhere volumetrically incompressible. We characterize the average orientation of an asymmetric lipid molecule by a unit vector \mathbf{n} , referred to as a director. A neutral surface, by definition, is

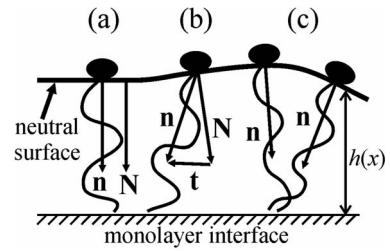


FIG. 2. Deformations of a monolayer. (a) The initial undeformed state of a monolayer is planar. The director, \mathbf{n} , and the normal, \mathbf{N} , are parallel to each other and perpendicular to the neutral surface. (b) Deformation of tilt. The director deviates from the normal by the tilt vector, \mathbf{t} . (c) Deformation of splay. Directors at adjacent points of the neutral surface deviate from each other but remain parallel to their corresponding normals (not shown). $h(x)$ is the distance between the monolayer interface and the neutral surface; it is referred to as the monolayer thickness.

the surface where the deformations of splay and area compression/stretching are independent of each other. As determined experimentally, it lies between the lipid polar headgroups and the hydrophobic tails at a distance of ~ 0.5 nm from the external surface [26]. The shape of the neutral surface is characterized by a unit normal vector \mathbf{N} directed into the monolayer, from headgroup to acyl chain. We refer to the distance $h(x)$ between the neutral surface and monolayer interface as the monolayer thickness (Fig. 2). All deformations are described by the vector fields of \mathbf{N} and \mathbf{n} on the neutral surface.

B. Deformations

We consider small deviations of a monolayer from its unperturbed state. In this state, the neutral surface is flat and all directors are parallel to each other and perpendicular to the neutral surface [Fig. 2(a)]. In continuum elastic theory of membranes, all perturbations of a membrane can be described by three independent deformations. These fundamental deformations and their elastic moduli are area lateral compression/stretching (K_a), splay (B), and tilt (k). For a typical lipid bilayer containing appreciable amounts of cholesterol $K_a \gg k$ and $K_a \gg B/h_m^2$ (where $h_m \sim 2$ nm is the monolayer thickness) [27] and, hence, the contributions of area compression/stretching can be neglected. In other words, the membrane is effectively unstretchable.

The deformation of tilt is characterized at every point on the neutral surface by the deviation of the director from the normal [Fig. 2(b)]. The tilt vector \mathbf{t} is given by $\mathbf{t} = \mathbf{n}(\mathbf{n} \cdot \mathbf{N}) - \mathbf{N}$. [28]. For a small deformation $\mathbf{t} \approx \mathbf{n} - \mathbf{N}$, and here the length of the tilt vector is numerically equal to the angle between the director and the normal.

The deformation of splay is given by $\text{div } \mathbf{n}$ along the neutral surface. That is, splay is the angle between the directors at adjacent points of the neutral surface [Fig. 2(c)] [28,29]. Expressing the director as $\mathbf{n} = \mathbf{t} + \mathbf{N}$, we obtain $\text{div } \mathbf{n} = \text{div } \mathbf{t} + \text{div } \mathbf{N} = \text{div } \mathbf{t} - J$, where $J \equiv -\text{div } \mathbf{N}$ is the geometric curvature of the neutral surface. Thus, the deformation of splay is a combination of nonuniform tilt and bending of the neutral surface.

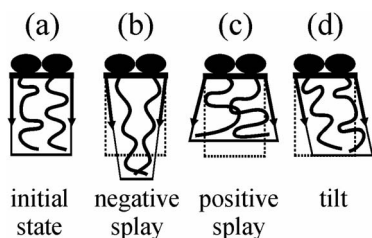


FIG. 3. Elastic deformations of an element of a volumetrically incompressible monolayer when the area of its neutral surface is constant. (a) The initial undeformed state. (b) Deformation of negative splay. The thickness of the monolayer must increase if the volume of the element and the area of the neutral surface are to be conserved. (c) Deformation of positive splay. This results in a decrease in monolayer thickness. (d) Deformation of tilt. Monolayer thickness is not altered. The dashed line indicates the initial shape of the monolayer element.

For a one-dimensional system, the vectors \mathbf{n} , \mathbf{N} , and \mathbf{t} depend only on the x coordinate. The monolayer can thus be described by the projections of these vectors onto the Ox axis (i.e., $n_x=n$, $N_x=N$, and $t_x=t$). For small deformations, the divergence along the neutral surface is the same as derivatives with respect to x , so $\text{div } \mathbf{n}=dn/dx$. In the initial flat state, the projections of all three vectors are everywhere equal to zero.

C. Volumetric incompressibility

The deformations are constrained for a volumetrically incompressible monolayer. For uniform tilt, the area of the neutral surface is constant and so the thickness of the monolayer must also remain constant [Fig. 3(d)]. Physically, the lipid tails elongate and approach each other as they incline. In contrast, for the splay deformation, the directors do not remain parallel so splay alters the monolayer thickness. Physically, the lipid tails elongate if directors incline toward each other and shorten if directors incline outward [Figs. 3(b) and 3(c)]. The condition of volumetric incompressibility can be written as:

$$h(x) = h - \frac{h^2}{2} n'(x) \text{ or } \xi(x) = h - h(x) = \frac{h^2}{2} n'(x), \quad (1)$$

where h (without the argument x) is the monolayer thickness in the initial state and the superscripted prime denotes a derivative with respect to x . It follows from Eq. (1) that tilt does not change monolayer thickness but splay does: for pure tilt, the orientation and length of \mathbf{n} is constant, so $n'=0$; for pure splay, $\text{div } \mathbf{n}=\text{const}$ and so $n' \neq 0$.

D. The energy of deformations

We calculate the elastic free energy, F , of a monolayer relative to the unperturbed flat state. Splay and tilt contribute quadratically with small deformations to yield:

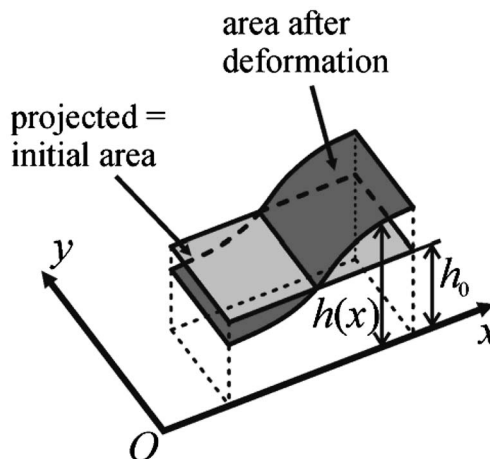


FIG. 4. The neutral surface of a monolayer in its initial planar state (light gray) and after deformation (dark gray). The neutral surface has a larger area after deformation than before. After deformation, the area of the neutral surface projects onto xy surface of the initial area.

$$F = \int \left(\frac{B}{2} (\text{div } \mathbf{n} + J_0)^2 - \frac{B}{2} J_0^2 + \frac{k}{2} \mathbf{t}^2 \right) dA + \sigma \delta A \quad (2)$$

where δA is the variation of the area of the neutral surface, J_0 is the spontaneous curvature of the monolayer, and σ is the lateral tension applied to the monolayer. Integration is performed over the entire neutral surface of the monolayer. The first two terms under the integral arise from the splay deformation and the third arises from tilt. The last term is the work that must be performed against the lateral tension to change the area of the neutral surface of the monolayer: At the boundary of two height-mismatched domains, the deformations cause the neutral surface to deviate from planar. The area of the neutral surface that is needed to cover the same projected area thus becomes larger (Fig. 4). Because we assume that the neutral surface is nonstretchable (i.e., the area per lipid remains constant), its area increases at the boundary by incorporation of additional lipids into the monolayer from regions far from the boundary. Work must be performed against the lateral tension σ if the area is to increase, as given by the last term in Eq. (2).

The assumption that the boundary of the raft remains straight yields that the area variation δA per unit length in the Oy direction is given by

$$\delta A = \int (\sqrt{1 + h'(x)^2} - 1) dx. \quad (3)$$

Expanding δA and dA into a Taylor series for small deformations ($h' \ll 1$) and truncating terms higher than needed for the required order of accuracy yields

$$\delta A = \int (\sqrt{1 + h'(x)^2} - 1) dx \approx \int \frac{1}{2} h'(x)^2 dx,$$

$$dA = \sqrt{1 + h'(x)^2} dx \approx dx. \quad (4)$$

By substituting $t = n - N \approx n - h'$ for the projection of the tilt vector, t , we can rewrite Eq. (2) to second order in deformations as

$$\begin{aligned} F &= \int \left\{ \frac{B}{2} [n'(x) + J_0]^2 - \frac{B}{2} J_0^2 + \frac{k}{2} [n(x) - h'(x)]^2 \right\} dx \\ &\quad + \sigma \int \frac{1}{2} h'(x)^2 dx \\ &= \int \left\{ \frac{B}{2} [n'(x) + J_0]^2 - \frac{B}{2} J_0^2 + \frac{k}{2} [n(x) - h'(x)]^2 \right. \\ &\quad \left. + \frac{\sigma}{2} h'(x)^2 \right\} dx. \end{aligned} \quad (5)$$

The condition of volumetric incompressibility [Eq. (1)] yields $h'(x) = n'' h^2 / 2$, which we substitute into Eq. (5) to express F as a function of only the directors $n(x)$ and their derivatives. After minimizing the functional Eq. (5) with respect to $n(x)$ we obtain the Euler-Lagrange equation,

$$h^4 \left(1 + 2 \frac{\sigma}{k} \right) n^{(4)}(x) + 4(h^2 - l^2) n''(x) + 4n(x) = 0 \quad (6)$$

or

$$m^4 n^{(4)}(x) + 4v^2 n''(x) + 4n(x) = 0, \quad (7)$$

where $m = h(1 + 2\sigma/k)^{1/4}$, $v = \sqrt{h^2 - l^2}$, $l = \sqrt{B/k}$.

III. SOLUTION OF THE PROBLEM

A. Energy of a semi-infinite monolayer with fixed boundary conditions

We first consider one semi-infinite monolayer (the surround, $x > 0$) that has a fixed director n_0 and a thickness deviation $\xi_0 = h - h(0)$ at its left boundary ($x = 0$). Because the system is translationally invariant along the boundary (i.e., along the Oy axis), we can rewrite Eq. (5) for the energy per unit length of boundary as

$$\begin{aligned} W &= \int_0^{+\infty} \left\{ \frac{B}{2} [n'(x) + J_0]^2 - \frac{B}{2} J_0^2 + \frac{k}{2} [n(x) - h'(x)]^2 \right. \\ &\quad \left. + \frac{\sigma}{2} h'(x)^2 \right\} dx. \end{aligned} \quad (8)$$

Solving Eq. (6) for the surround yields

$$n(x) = e^{-ax} \left(\frac{an_0 + \frac{2}{h^2} \xi_0}{b} \sin(bx) + n_0 \cos(bx) \right), \quad (9)$$

where

$$a = \sqrt{\frac{m^2 - v^2}{m^4}}, \quad b = \sqrt{\frac{m^2 + v^2}{m^4}}. \quad (10)$$

Inspection of Eq. (9) shows that the parameter a is the inverse of the characteristic length of the decay of the defor-

mations and b is the inverse characteristic length of their oscillation. We use the volumetric incompressibility condition Eq. (1), substitute $n(x)$ from Eq. (9) into the functional Eq. (8), and integrate to obtain

$$W = -kl^2 n_0 J_0 + k \left(\frac{am^2}{2} n_0^2 + \left(\frac{m^2}{h^2} - 1 \right) n_0 \xi_0 + \frac{am^4}{h^4} \xi_0^2 \right). \quad (11)$$

For $\sigma = 0$, $m = h$, $a = l/h^2$, and $b = \sqrt{2h^2 - l^2}/h^2$, the energy per unit length Eq. (11) is

$$W = -kl^2 n_0 J_0 + \frac{kl}{2} \left(n_0^2 + \frac{2}{h^2} \xi_0^2 \right). \quad (12)$$

B. Line tension

We now consider the entire system of the raft and surround (Fig. 1) in order to determine the line tension. We denote variables referring to the raft by the index r and for the surround by the index s . The energy per unit length of the boundary Eq. (11) is

$$W_s = -k_s l_s^2 n_0 J_s + k_s \left(\frac{a_s m_s^2}{2} n_0^2 + \left(\frac{m_s^2}{h_s^2} - 1 \right) n_0 \xi_s + \frac{a_s m_s^4}{h_s^4} \xi_s^2 \right) \quad (13)$$

in the surround, and is

$$W_r = k_r l_r^2 n_0 J_r + k_r \left(\frac{a_r m_r^2}{2} n_0^2 - \left(\frac{m_r^2}{h_r^2} - 1 \right) n_0 \xi_r + \frac{a_r m_r^4}{h_r^4} \xi_r^2 \right) \quad (14)$$

in the raft. The total energy per unit length of the boundary is

$$W_0 = W_s + W_r. \quad (15)$$

At the boundary, the thickness deviations, ξ_r and ξ_s , must satisfy the condition that the monolayer thickness $h(x)$ is continuous [25]. This condition can be written in the following forms:

$$\begin{aligned} h(0) &= h_s - \xi_s = h_r - \xi_r, \quad \text{or equivalently,} \quad \xi_s = \xi_r - (h_r - h_s) \\ &= \xi_r - \delta. \end{aligned} \quad (16)$$

By substituting ξ_s into Eq. (15) and minimizing the total energy over n_0 and ξ_r , we obtain our final expression for the line tension.

Lipid bilayer membranes can only sustain lateral tensions of at most 5–10 mN/m before they rupture [30]. Therefore σ is typically much smaller than the tilt elastic modulus $k \sim 40$ mN/m. The exact values of elastic moduli of rafts are unknown, but it is very likely that they are equal to or larger than those of a surround [27]. Assuming $\sigma \ll k$, the Taylor series of the right-hand side of Eq. (15) can be truncated beyond the linear term in σ [see Eqs. (7) and (10)]; for $h_r - h_s = \delta$, $\delta \ll h_0$, and $h_r \sim h_s \sim h_0$, the Taylor series of Eq. (15) can be truncated beyond the quadratic term in δ . Carrying out the minimization procedure on Eq. (15) and truncating the Taylor series as described, we obtain the dependence of

line tension to first order in σ and second order in δ :

$$\gamma = \gamma_0 + \frac{\sigma}{(k_r l_r + k_s l_s)^2} \left\{ \left(\frac{k_r^2 l_r^3 + k_s^2 l_s^3}{2l_r l_s} + \frac{l_r l_s (k_r^2 l_r + k_s^2 l_s)}{h_0^2} \right) \delta^2 + (k_r l_r + k_s l_s) \Delta J \delta + \frac{(l_r + l_s) h_0^2}{4l_r l_s} (\Delta J)^2 \right\}, \quad (17)$$

where $\gamma_0 = [k_r k_s l_r l_s \delta^2 / (k_r l_r + k_s l_s) h_0^2] - [\Delta J^2 / 2(k_r l_r + k_s l_s)]$, $\Delta J = k_r l_r^2 J_r - k_s l_s^2 J_s = B_r J_r - B_s J_s$.

IV. RESULTS

A. Line tension depends on lateral tension

From Eq. (17), we obtain the linear contribution of lateral tension to line tension, γ_σ , for $\sigma \ll k$,

$$\gamma_\sigma = \frac{\sigma}{(k_r l_r + k_s l_s)^2} \left\{ \left(\frac{k_r^2 l_r^3 + k_s^2 l_s^3}{2l_r l_s} + \frac{l_r l_s (k_r^2 l_r + k_s^2 l_s)}{h_0^2} \right) \delta^2 + (k_r l_r + k_s l_s) \Delta J \delta + \frac{(l_r + l_s) h_0^2}{4l_r l_s} (\Delta J)^2 \right\}, \quad (18)$$

The expression in brackets in Eq. (18) is quadratic in the variables δ and ΔJ . Although ΔJ can be negative, the Sylvester criterion for positive-definiteness shows that the term within brackets is positive for all physical values of parameters (see Appendix). Thus, the application of lateral tension always increases line tension. Equation (18) is the work that must be performed against lateral tension in order to create the difference between the projected area and the actual area after deformation of the neutral surface within the proximity of the boundary (Fig. 4).

B. Elastic moduli of raft and surround membrane

Values of elastic moduli depend on membrane composition. For typical surrounds, the splay modulus varies in the range of 5–20 kT/monolayer [31] (kT $\sim 4 \times 10^{-20}$ J); we use $B \sim 10$ kT for purposes of illustration. It has been argued on theoretical grounds that the tilt modulus of a monolayer should be well approximated by the surface tension of a hydrocarbon/water interface (i.e., $k \sim 40$ mN/m) [28,32,33], and this approximation has been used to quantitatively account for experimental data [33]. The elastic moduli for rafts are unknown. The splay moduli of membranes with high cholesterol content are two to three times larger than for membranes not containing cholesterol [27], but a high content of cholesterol increases the splay modulus of membranes in the H_{II} phase by only 30–40% [34]. If the tilt modulus can be estimated from the surface tension of a hydrocarbon/water interface, it should be roughly the same for a raft and a surround. In view of the uncertain elastic moduli, we consider three cases.

In the first, we consider a “soft” raft where $B_r = B_s = B = 10$ kT and $k_r = k_s = k = 40$ mN/m. The line tension is

$$\gamma_{soft} = \frac{kl}{2h_0^2} \delta^2 - \frac{kl^3}{4} (J_r - J_s)^2 + \sigma \left(\frac{h_0^2 + 2l^2}{4h_0^2 l} \delta^2 + \frac{l}{2} (J_r - J_s) \delta + \frac{lh_0^2}{8} (J_r - J_s)^2 \right), \quad l = \sqrt{\frac{B}{k}}. \quad (19)$$

For the second case, we describe a “firm” raft by $B_r = 4B_s = 4B = 40$ kT and $k_r = k_s = k = 40$ mN/m; the line tension is

$$\gamma_{firm} = \frac{2kl}{3h_0^2} \delta^2 - \frac{kl^3}{6} (4J_r - J_s)^2 + \sigma \left(\frac{8l^2 + 3h_0^2}{12h_0^2 l} \delta^2 + \frac{l}{3} \delta (4J_r - J_s) + \frac{lh_0^2}{24} (4J_r - J_s)^2 \right). \quad (20)$$

In the last case, we consider a “rigid” raft where $B_r = 4B_s = 4B = 40$ kT, $k_r = 4k_s = 4k = 160$ mN/m; the line tension is

$$\gamma_{rigid} = \frac{4kl}{5h_0^2} \delta^2 - \frac{kl^3}{10} (4J_r - J_s)^2 + \sigma \left(\frac{17(2l^2 + h_0^2)}{50h_0^2 l} \delta^2 + \frac{l}{5} \delta (4J_r - J_s) + \frac{lh_0^2}{50} (4J_r - J_s)^2 \right). \quad (21)$$

C. Line tension for $\Delta J = 0$

Line tension generally depends on the spontaneous curvatures of the raft and surrounding monolayers. For the specific case that spontaneous curvature does not contribute to line tension (i.e., $\Delta J = k_r l_r^2 J_r - k_s l_s^2 J_s = 0$), we have

$$\gamma = \gamma_0 + \frac{\sigma \delta^2}{(k_r l_r + k_s l_s)^2} \left(\frac{k_r^2 l_r^3 + k_s^2 l_s^3}{2l_r l_s} + \frac{l_r l_s (k_r^2 l_r + k_s^2 l_s)}{h_0^2} \right), \quad (22)$$

where $\gamma_0 = (k_r k_s l_r l_s / k_r l_r + k_s l_s) (\delta^2 / h_0^2)$ is the line tension for $\sigma = 0$. For a soft raft, Eq. (22) becomes

$$\gamma = \frac{\sqrt{Bk} \delta^2}{2 h_0^2} + \frac{\sqrt{Bk} \delta^2}{2 h_0^2} \sigma \left(\frac{1}{2B/h_0^2} + \frac{1}{k} \right). \quad (23)$$

The application of a lateral tension alters both the splay and tilt deformations. These changes are described by the two terms in the parenthesis in Eq. (23). The first term arises from the influence of lateral tension on splay deformations near the boundary, and the second one arises from its influence on tilt deformations. As is readily seen, if a deformation cannot occur (i.e., $B \rightarrow \infty$ eliminating any splay or $k \rightarrow \infty$ eliminating any tilt), the corresponding term reduces to zero.

We illustrate the dependence of the line tension of a raft in a bilayer, 2γ , on the lateral tension, 2σ , for soft, firm, rigid, and perfectly rigid rafts (Fig. 5). The slopes of all lines are positive. The slight increase in slope as the raft becomes more rigid illustrates that line tension increases more steeply with lateral tension for a rigid than for a soft raft. As can be appreciated from Eq. (18), the slope also increases if δ becomes greater or h_0 becomes smaller.

D. Line tension for nonzero spontaneous curvatures

The spontaneous curvatures of a raft and a surround are generally neither equal to each other nor equal to zero. We

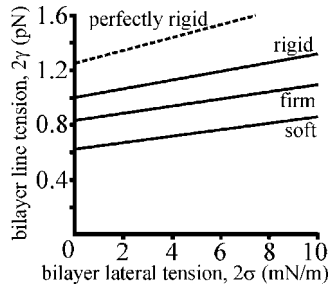


FIG. 5. Dependence of bilayer line tension, 2γ (in pN), on bilayer lateral tension, 2σ (in mN/m), for a soft, firm, rigid, and perfectly rigid raft. Here and for Figs. 6 and 7, $B=10$ kT, $k=40$ mN/m, $h_0=2$ nm, and $\delta=0.25$ nm. For this figure, $J_r=0$ and $J_s=0$.

illustrate the dependence of raft line tension, 2γ , on bilayer lateral tension, 2σ , for $J_r=+1/20$ nm $^{-1}$ and $J_s=-1/20$ nm $^{-1}$ for soft, firm, and rigid rafts (Fig. 6). The slopes of these lines are greater for $J_r>J_s$ than for $J_r=J_s=0$ (Fig. 5). The reason for these slope dependencies can be appreciated by inspecting Eq. (18). When $J_r=J_s=0$, lateral tension contributes through a single term proportional to δ^2 . When $J_r>J_s$, two additional positive terms contribute, so lateral tension has a greater affect on line tension. For bilayers composed of cholesterol, 1,2-dipalmitoyl-*sn*-glycero-3-phosphocholine (DPPC) (a saturated lipid), and 1,2-dioleoyl-*sn*-Glycero-3-phosphocholine (DOPC) (an unsaturated lipid), the DPPC is enriched within the raft phase and DOPC is depleted [20]. Both acyl chains of DPPC are saturated whereas those of DOPC are monounsaturated, so DPPC should have a more positive spontaneous curvature than DOPC. A raft and surround contain approximately the same percentage of cholesterol, so the spontaneous curvature of a raft should be more positive than that of surround (i.e., $J_r>J_s$). The same situation should apply to membranes containing sphingomyelin in place of DPPC because they have the same headgroup and sphingomyelin also has saturated acyl chains. (These expectations of spontaneous curvature have not yet been experimentally explored.) Because it is most likely that $J_r>J_s$, we expect that the line tension of a raft would exhibit the strong dependence on applied lateral tension that is illustrated in Fig. 6.

We can also consider the case $J_r<0<J_s$. Here, the slopes and the increase in slope with the firmness of the raft (Fig. 7) are less than for $\Delta J=0$ (Fig. 5). This readily follows from

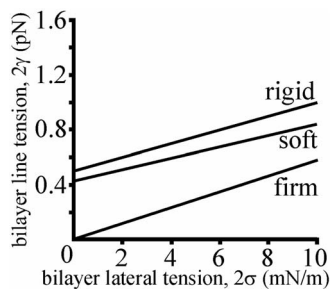


FIG. 6. Dependence of bilayer line tension, 2γ (in pN), on bilayer lateral tension, 2σ (in mN/m), for a soft, firm, and rigid raft. Here, $J_r=+1/20$ nm $^{-1}$ and $J_s=-1/20$ nm $^{-1}$.

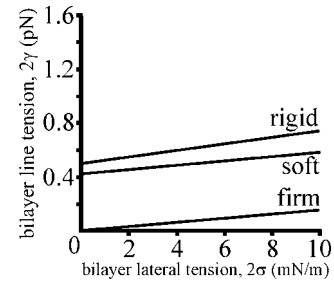


FIG. 7. Dependence of bilayer line tension, 2γ (in pN), on bilayer lateral tension, 2σ (in mN/m), for a soft, firm, and rigid raft. $J_r=-1/20$ nm $^{-1}$ and $J_s=+1/20$ nm $^{-1}$.

Eq. (18), because for $J_r<0<J_s$ the term proportional to $\delta(k_r J_r^2 J_r - k_s J_s^2 J_s) = B_r J_r - B_s J_s$ is negative for all values of splay moduli, and so lateral tension makes less of a contribution to line tension. In contrast, if $0<J_r<J_s$, then $\Delta J = B_r J_r - B_s J_s$ can be either positive or negative when $B_r > B_s$, and so the cross term ($\sim \delta \Delta J$) can have either sign.

V. DISCUSSION

In the present study we have calculated the consequence of applied lateral tension on the interfacial energy, or equivalently, the line tension, between a raft and a surround. We have shown that if line tension is due to height mismatch between the raft and surround, the application of lateral tension must cause the line tension to increase. The amount of the increase strongly depends on the values and signs of the spontaneous curvatures of the raft and the surrounding membrane. Height mismatch and spontaneous curvatures are determined by lipid composition. In our model, contributions to line tension caused by interactions between lipids, such as chemical or Van der Waals forces, are ignored, but a relatively small height mismatch, on the order of 0.5 nm for a bilayer, should dominate the consequences of these interactions on line tension [25]. Thus, our model should be applicable for quantitatively determining the values of line tension over a wide range of lipid compositions.

Equation (18) is the central result of this study, because it provides the means to calculate the contribution of lateral tension to line tension γ_σ as a function of the spontaneous curvatures of the raft and surround. We now consider the three terms in this equation. Because we considered small deformations, we calculated the elastic energy up to, and including, all quadratic terms. One term in Eq. (18) is proportional to δ^2 and another is proportional to ΔJ^2 ; these two terms are obviously always positive. But the cross term, proportional to $\delta \Delta J$, can be either positive or negative. We show in the Appendix that according to the Sylvester criterion, the sum of the three terms of Eq. (18) is always positive. Thus, the application of lateral tension always increases the total energy of deformation at the raft boundary, or, equivalently, always increases the line tension. What is the physical origin of the two quadratic terms?

In order to consider the role of δ , let $\Delta J=0$ but $\delta \neq 0$. After the elastic deformations of a monolayer compensate for the hydrophobic mismatch, the neutral surfaces of the raft and

the surround deviate from their initial planar state, and so the area of the deformed neutral surface is larger than the initial onto which it projects. Work must be expended against the applied lateral tension to provide this increase in area. For small deformations, the amplitude of the deformation that compensates the hydrophobic mismatch should be proportional to δ , but the contribution of lateral tension to the line tension should not depend on whether the raft is thicker (i.e., $\delta > 0$) or thinner (i.e., $\delta < 0$) than the surround. Thus, the contribution should be proportional to δ^2 . In our second-order approximation, this is the simplest dependence on δ that is independent of the sign of δ .

When $\Delta J = 0$, not only should the contribution of the lateral tension to line tension γ_σ be proportional to δ^2 , but the total line tension, γ [Eq. (17)], should be as well. Consider the following process. Initially the raft and surround monolayers have the same thickness ($\delta = 0$), but they can have different elastic moduli. A deformation does not occur, so the line tension, γ , is equal to zero. Now, let the thickness of raft increase while the thickness of surround is maintained (i.e., let $\delta > 0$). Elastic deformations (with amplitude proportional to δ) appear and γ increases. If instead the thickness of the raft were to decrease (i.e., $\delta < 0$), the line tension would still increase in exactly the same manner. Because line tension should not depend on the sign of the height mismatch, the total line tension, γ , should be proportional to δ^2 . (This can be quantitatively seen from Eq. (17) by letting $\Delta J = 0$, $\delta \neq 0$ and noting the form of the first term in γ_0 and the first term in brackets.)

To consider the third term in Eq. (18), which is proportional to ΔJ^2 , we set $\delta = 0$ and $\Delta J \neq 0$. Two phenomena need to be considered. The first arises because if $\Delta J \neq 0$, the membrane is under mechanical stress in its initial planar state. The partial relaxation in stress after the monolayers elastically deform near the boundary contributes a negative energetic term that is independent of the sign of ΔJ . This term is thus proportional to $-(\Delta J)^2$ up to quadratic order. The second phenomenon appears because, in increasing the area of the neutral surface, the deformations must work against lateral tension. This requires positive work that depends only on the extent of the area increase. Because the exact shape of the neutral surface is not relevant, this energy is independent of the sign of ΔJ . That is, this contribution to energy is proportional to $+(\Delta J)^2$. In Eq. (17) for total line tension, γ , the second negative term in γ_0 is a consequence of the relaxation of stress and the third positive term in the brackets in γ_σ arises from the work against lateral tension.

The physical meaning of the cross term is as follows: Because the raft and surround thicknesses are different, application of a lateral tension results in a torque at the boundary that causes the boundary director n_0 to slightly rotate counterclockwise (if the raft is on the left and the surround is on the right)—see Fig. 8. If the surround is made to have a more positive spontaneous curvature (e.g., by addition of a positive curvature lipid that preferentially partitions into the surround), ΔJ ($\Delta J = B_r J_r - B_s J_s$) becomes more negative. As a result of the applied tension rotating the boundary director, the splay in the surround becomes closer to its spontaneous splay. This decreases the stresses and lessens the total work expended against the lateral tension. In the opposite case, we

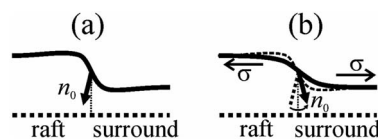


FIG. 8. Application of lateral tension results in rotation of the boundary director, n_0 . (a) The orientation of the boundary director before the application of lateral tension. (b) The application of the lateral tension, σ , causes the boundary director to rotate counterclockwise.

add negative curvature to the surround (e.g., add a lipid to the surround with a narrow head group and wide tail, $\Delta J > 0$). Now the counterclockwise rotation of the boundary director n_0 causes the splay to increase its deviation of curvature further away from the spontaneous curvature. This increases the stress and thus leads to greater work expended against lateral tension. The asymmetry in the direction of the stress with respect to the sign of the spontaneous curvature is accounted for solely by the cross term. When the cross term is positive, lateral tension makes a greater positive contribution to the line tension (Fig. 6) than when the cross term is negative (Fig. 7).

The value of line tension of a raft in a membrane may be of biological importance. The decrease in interfacial free energy upon merger of rafts promotes merger; this decrease competes with the increase in entropic free energy caused by the reduction in the number of rafts. Consequently, line tension influences the size distribution of a raft ensemble: at equilibrium, rafts should have merged into one domain for a high value of line tension, whereas a dispersion of many nanodomains should coexist for low values of line tension. In fact, there exists a critical line tension, γ_c , such that rafts merge for $\gamma > \gamma_c$ and remain dispersed for $\gamma < \gamma_c$ [23]. (The value of γ_c depends on lipid composition.) Based on the demonstration that line tension increases as the applied lateral tension is made greater, we predict that an ensemble of rafts in a membrane, dispersed in submicroscopic resolution sizes in the absence of lateral tension, would merge to create microscopically observable rafts of several micrometers upon application of significant lateral tension. We have experimentally found, using GUVs, that this is the case [Ayuyan and Cohen, unpublished]. In the case of biological cells, lateral tension is generated by interactions between the plasma membrane and underlying cytoskeleton [35,36]. These interactions can and do vary, and variation in local lateral tension is thought to regulate some membrane processes such as endocytosis [37–39]. It may be that cells regulate raft size through the dependence of line tension on lateral tension—an increase in local lateral tension may promote raft merger.

ACKNOWLEDGMENTS

We thank Prof. Yuri Chizmadzhev and Dr. Artem Ayuyan for continual advice and encouragement in this study. This work was supported by grants from the Program for Molecular and Cellular Biology of the Russian Academy of Sciences, the Russian Foundation for Basic Research (No. 05-

04-49624), the Civilian Research and Development Foundation Grant Assistance Program (No. RUB1-1297(5)-MO-05), and the National Institutes of Health (No. R01 GM066837).

APPENDIX

Equation (18) yields the contribution of lateral tension upon line tension. We rewrite it as

$$\gamma_\sigma = \frac{\sigma}{(k_r l_r + k_s l_s)^2} (a \delta^2 + 2b \delta \Delta J + c \Delta J^2), \quad (\text{A1})$$

where

$$a = \frac{k_r^2 l_r^3 + k_s^2 l_s^3}{2l_r l_s} + \frac{l_r l_s (k_r^2 l_r + k_s^2 l_s)}{h_0^2}$$

$$b = \frac{k_r l_r + k_s l_s}{2}$$

$$c = \frac{(l_r + l_s) h_0^2}{4l_r l_s}.$$

Because the term within the parentheses has a quadratic form, it is positive if and only if $ca - b^2 > 0$. In our case

$$ca - b^2 = \frac{1}{8} (l_r + l_s) (k_r^2 l_r^3 + k_s^2 l_s^3) \left(\frac{h_0}{l_s l_r} \right)^2 + \frac{1}{4} l_r l_s (k_r - k_s)^2 \quad (\text{A2})$$

is always positive because l_r and l_s are positive. It thus follows from the Sylvester criterion [40] that the right-hand side of Eq. (A1) is positive definite.

-
- [1] C. Leidy, L. Linderoth, T. L. Andresen *et al.*, *Biophys. J.* **90**, 3165 (2006).
- [2] J. Ren, S. Lew, J. Wang *et al.*, *Biochemistry* **38**, 5905 (1999).
- [3] P. W. Janes, S. C. Ley, and A. I. Magee, *J. Cell Biol.* **147**, 447 (1999).
- [4] W. Zhang, J. Sloan-Lancaster, J. Kitchen *et al.*, *Cell* **92**, 83 (1998).
- [5] W. Zhang, R. P. Tribble, and L. E. Samelson, *Immunity* **9**, 239 (1998).
- [6] A. V. Samsonov, I. Mihalyov, and F. S. Cohen, *Biophys. J.* **81**, 1486 (2001).
- [7] A. Pralle, P. Keller, E.-L. Florin *et al.*, *J. Cell Biol.* **148**, 997 (2000).
- [8] K. Simons and E. Ikonen, *Nature (London)* **387**, 569 (1997).
- [9] E. D. Sheets, D. Holowka, and B. Baird, *J. Cell Biol.* **145**, 877 (1999).
- [10] T. Harder, *Curr. Opin. Immunol.* **16**, 353 (2004).
- [11] M. Fabbri, S. Di Meglio, M. C. Gagliani *et al.*, *Mol. Biol. Cell* **16**, 5793 (2005).
- [12] V. M. Pietiainen, V. Marjomaki, J. Heino *et al.*, *Ann. Med.* **37**, 394 (2005).
- [13] R. G. Parton and A. A. Richards, *Traffic (Oxford, U. K.)* **4**, 724 (2003).
- [14] M. Bagnat, S. Keranen, A. Shevchenko *et al.*, *Proc. Natl. Acad. Sci. U.S.A.* **97**, 3254 (2000).
- [15] E. T. Spiliotis, T. Pentcheva, and M. Edidin, *Mol. Biol. Cell* **13**, 1566 (2002).
- [16] H. A. Rinia, M. M. Snel, J. P. van der Eerden *et al.*, *FEBS Lett.* **501**, 92 (2001).
- [17] J. C. Lawrence, D. E. Saslowsky, J. M. Edwardson *et al.*, *Biophys. J.* **84**, 1827 (2003).
- [18] S. A. Akimov, P. I. Kuzmin, J. Zimmerberg *et al.*, *J. Electroanal. Chem.* **564**, 13 (2004).
- [19] C. B. Yuan and L. J. Johnston, *Biophys. J.* **79**, 2768 (2000).
- [20] S. L. Veatch, I. V. Polozov, K. Gawrisch *et al.*, *Biophys. J.* **86**, 2910 (2004).
- [21] J. Pencer, T. Mills, V. Anghel *et al.*, *Eur. Phys. J. E* **18**, 447 (2005).
- [22] J. R. Silvius, *Biophys. J.* **85**, 1034 (2003).
- [23] V. A. J. Frolov, Y. A. Chizmadzhev, F. S. Cohen *et al.*, *Biophys. J.* **91**, 189 (2006).
- [24] T. Baumgart, S. T. Hess, and W. W. Webb, *Nature (London)* **425**, 821 (2003).
- [25] P. I. Kuzmin, S. A. Akimov, Y. A. Chizmadzhev *et al.*, *Biophys. J.* **88**, 1120 (2005).
- [26] M. M. Kozlov, S. Leikin, and R. P. Rand, *Biophys. J.* **67**, 1603 (1994).
- [27] E. Evans and W. Rawicz, *Phys. Rev. Lett.* **64**, 2094 (1990).
- [28] M. Hamm and M. M. Kozlov, *Eur. Phys. J. E* **3**, 323 (2000).
- [29] Y. Kozlovsky and M. M. Kozlov, *Biophys. J.* **82**, 882 (2002).
- [30] E. Evans, V. Heinrich, F. Ludwig *et al.*, *Biophys. J.* **85**, 2342 (2003).
- [31] W. Rawicz, K. C. Olbrich, T. McIntosh *et al.*, *Biophys. J.* **79**, 328 (2000).
- [32] F. S. Cohen and G. B. Melikyan, *J. Membr. Biol.* **199**, 1 (2004).
- [33] M. Hamm and M. M. Kozlov, *Eur. Phys. J. B* **6**, 519 (1998).
- [34] Z. Chen and R. P. Rand, *Biophys. J.* **73**, 267 (1997).
- [35] M. P. Sheetz, J. E. Sable, and H. G. Dobereiner, *Annu. Rev. Biophys. Biomol. Struct.* **35**, 417 (2006).
- [36] I. Titushkin and M. Cho, *Biophys. J.* **90**, 2582 (2006).
- [37] J. Dai, H. P. Ting-Beall, and M. P. Sheetz, *J. Gen. Physiol.* **110**, 1 (1997).
- [38] C. E. Morris and U. Homann, *J. Membr. Biol.* **179**, 79 (2001).
- [39] G. Apodaca, *Am J Physiol Renal Physiol* **282**, F179 (2002).
- [40] V. M. Volosov and I. G. Volosova, translated by A. D. Myškis, *Advanced Mathematics for Engineers* (MIR Publishers, Moscow, 1975).